DINAME 2023 - Proceedings of the XIX International Symposium on Dynamic Problems of Mechanics,
A.S. De Paula, A.T. Fabro and M.R. Machado (Editors), ABCM.
Pirenópolis, Go, Brazil, February 26th to March 3rd, 2023

# Experimental Estimation of Brake Pad Wear for Passenger Cars Based on Longitudinal Dynamics

**Kenneth Jensen**[1], **Ilmar Santos**[1], **Line Clemmensen**[2], **and Søren Theodorsen**[3]

[1] Department of Civil and Mechanical Enginnering, Technical University of Denmark, kemje@dtu.dk / ilsa@dtu.dk

[2] Department of Applied Mathematics and Computer Science, Technical University of Denmark, lkhc@dtu.dk

[3] ILIAS Solutions, Brussels, Belgium, soren.theodorsen@ilias-solutions.com

*Abstract: This paper considers the problem of estimating brake pad wear of a passenger car, based on usage data and vehicle longitudinal dynamics. To broaden the applicability of the proposed methods, only basic usage data is considered, using inertial measurement unit (IMU), global navigation satellite system (GNSS), and standard vehicle on-board diagnostics (OBD) data. This excludes the use of manufacturer specific vehicle data. The paper considers the following problems: (I) estimation of vehicle drag, (II) estimation of engine braking, (III) prediction of vehicle braking state, and (IV) estimation of brake pad wear. Results from (I) and (II) are used for (III), predicting the braking state by comparing measured vehicle acceleration with accelerations estimated from longitudinal dynamics. The brake pad wear is estimated using linear regression with a single feature: the product of distance travelled and estimated longitudinal braking force during braking. Data was sampled from a modern passenger car, for fitting and validation of models. For the wear estimation (IV), the thickness of a brake pad of the car was measured. A total of 16 measurements over the course of approximately 5,000 km were carried out. The drag and engine braking estimates from (I) and (II) show good agreements with measurements. The predicted braking states were also validated experimentally, using object tracking of the brake pedal. Finally, the linear regression model appears to indicate an almost linear relation between the used feature and the measured wear with a* $R^2 = 0.97$.

***Keywords: Wear prediction, longitudinal dynamics, parameter estimation, maintenance, experimental validation***

## INTRODUCTION

Braking systems are critical for ensuring safe operation of cars, allowing them to slow down in a controllable manner. Disc brakes are the most common choice of brake type employed on modern passenger cars, offering a higher tolerance for high temperatures and more linear and predictable operation than drum brakes (Limpert, 2011, ch. 2). A disc brake consists of a disc mounted to the rotating wheel hub, usually made of cast iron or composite material, as well as a pair of brake pads. The pads are mounted such that they clamp the disc by a force applied by one or more hydraulic pistons. The friction between the disc and pads then generates a braking torque, converting the vehicle kinetic energy into heat. This also causes the disc and pads to wear down over time, with pads generally wearing down at a higher rate. The useful life of brake pads is sometimes specified in terms of mileage, this does however not take driving behaviour into consideration. As such, condition monitoring is performed by physical inspections, as well as by the use of wear indicators which function by alarming the driver when a certain wear has been reached. To improve upon this and reduce the amount of physical inspections, it is desirable to be able to predict wear of brake pads from vehicle usage. Such predictive maintenance would then also allow for smarter service scheduling and allocation of resources, especially relevant within fleet management. Some authors use simulation software to estimate wear (Zhang *et al.*, 2019; Rajesh *et al.*, 2019), while others investigate brake pad wear experimentally using test rigs (Tiedemann *et al.*, 2020; Kijanski *et al.*, 2020). Gailis and Berjoza (2012) investigate brake pad wear of cars under real-world conditions, attempting to correlate wear with mileage, but with limited success.

This paper follows the principles of Jensen *et al.* (2022b), restricting the use of manufacturer specific data from the controller area network (CAN-bus), allowing for application of developed methods to a broad range of vehicles. The significance of the paper then lies in the use of only easily attainable vehicle usage data for brake pad wear estimation. Considered data includes inertial measurement unit (IMU), global navigation satellite system (GNSS), and vehicle on-board diagnostics (OBD-II). All modern passenger cars are equipped with OBD-II, giving access to data such as vehicle and engine speeds. Validation is carried out with usage and wear data from a car under real-world conditions, with brake pad wear measured directly. For accurate brake pad wear estimation, it is first required to know when the brakes are being used, which is not available as a standard OBD-II parameter and must instead be predicted. This will be done by comparing estimated vehicle deceleration with measured decelerations. Decelerations will be estimated from vehicle longitudinal dynamics (Gillespie, 1992, ch. 2). This requires characterization of the vehicle dynamics, which will be done by use of coast-down tests (White and Korst, 1972), both with and without drivetrain engaged. The drivetrain affects the vehicle deceleration due to the engine braking torque, especially in lower gears where the torque is amplified significantly (Cliff and Bowler, 1998; White *et al.*, 2012). The engine braking torque will be estimated from OBD-II engine data using

polynomial expressions (Hendricks and Sorenson, 1990). Based on braking force estimated from vehicle longitudinal dynamics, wear is then estimated during braking based on the Archard (1953) wear model. While wear of brake pads increases with temperature (Liu and Rhee, 1978; Kijanski *et al.*, 2020), temperature effects will not be considered.

## MATHEMATICAL MODELLING

### Longitudinal dynamics model

The vehicle longitudinal dynamics can be expressed as in Eq. (1). Here $\dot{x}$ and $\ddot{x}$ is the longitudinal vehicle speed and acceleration respectively. Vehicle mass is given by $m$, effective tire radius $r$, engine torque $T_e$, drivetrain efficiency $\eta_{dt}$, ambient air density $\rho_a$, the product of aerodynamic drag coefficient and frontal area $C_a = C_d A_0$, gravitational acceleration $g$, rolling resistance coefficient $C_r$, and road gradient $\alpha$. The mass moment of inertia of the engine $I_e$ includes all contributions up to the transmission. The mass moment of inertia of the wheels $I_w$ is the total of all four wheels. The effective gearing $G$ is defined in Eq. (2) with differential gearing ratio $i_d$, and transmission gearing ratio $i_{t,j}$ for gear $j$.

$$\underbrace{\left(m + I_w \frac{1}{r^2} + I_e G^2\right)}_{\text{Inertia}} \ddot{x} = \underbrace{\eta_{dt} T_e G}_{\text{Engine}} - \underbrace{f(p_{\text{brake}})}_{\text{Friction brakes}} - \underbrace{\frac{1}{2}\rho_a C_a \dot{x}^2}_{\text{Aerodynmaic drag}} - \underbrace{mgC_r \cos(\alpha)}_{\text{Rolling resistance}} - \underbrace{mg \sin(\alpha)}_{\text{Gravitational}} \tag{1}$$

$$G = \frac{i_{t,j} i_d}{r} \tag{2}$$

### Vehicle Braking State

In order to predict when the brakes are being applied, the friction brake term is neglected for now and it is assumed that the throttle pedal is not being pressed such that $T_e \leq 0$. Because the friction brakes can only slow down the vehicle, it is assumed that if the measured deceleration is greater than estimated deceleration, the difference is caused by the application of the friction brakes. From the longitudinal dynamics in Eq. (1) the acceleration during coasting can then be written as Eq. (3). Based on this expression the vehicle braking state is to be predicted using Eq. (4). Considering that the acceleration is negative during braking, the vehicle is assumed to be braking if the difference between measured acceleration and estimated coasting acceleration is below some value $\beta$.

$$a_{\text{cst,esti}} = \frac{\eta_{dt} T_e G - \frac{1}{2}\rho_a C_a \dot{x}^2 - mgC_r \cos(\alpha) - mg \sin(\alpha)}{m + I_w \frac{1}{r^2} + I_e G^2} \tag{3}$$

$$\text{Braking state:} \quad B = \begin{cases} (0) \text{ Not braking} & \text{if} \quad a_{\text{meas}} - a_{\text{cst,esti}} > \beta \\ (1) \text{ Braking} & \text{if} \quad a_{\text{meas}} - a_{\text{cst,esti}} \leq \beta \end{cases} \tag{4}$$

The parameter $\beta$ is a constant used to control the sensitivity of the predictions and can be estimated by considering a binary classification, seeking to minimize the number of misclassifications on a data set with labels of when the vehicle is braking. The classification problem can be solved by considering the logistic regression model in Eq. (5), with a single feature $\Delta a = a_{\text{meas}} - a_{\text{cst,esti}}$.

$$p(Z) = \frac{1}{1 + \exp(-Z)} \quad , \quad Z = \theta_1 \Delta a + \theta_0 \tag{5}$$

The probability of braking and not braking is expressed by $p(Z)$, with the boundary then assumed to be $p(Z) = 0.5$. This means that if $p(Z) > 0.5$ then the vehicle is assumed to be braking. The problem is solved by finding the parameters $\theta_0$ and $\theta_1$ that minimizes some criteria e.g., the number of misclassification. After having found the optimal parameters, the expression in Eq. (5) can then be rearranged into Eq. (6), where the threshold $\beta$ appears.

$$\begin{aligned} p(Z) &= \frac{1}{1 + \exp(-\theta_1 \Delta a - \theta_0)} = 0.5 \\ &\Rightarrow \theta_1 \Delta a + \theta_0 = 0 \\ &\Rightarrow \Delta a = a_{\text{meas}} - a_{\text{cst,esti}} = -\frac{\theta_0}{\theta_1} = -\beta \end{aligned} \tag{6}$$

### Parameter Estimation

Usage of the longitudinal dynamics model requires knowledge of various time varying signals and constant parameters. The road grade $\alpha$ is approximated by the vehicle pitch, which along with vehicle speed $\dot{x}$ and acceleration $\ddot{x}$ are provided

by a sensor fusion algorithm. IMU data is fused with GNSS positions and OBD-II vehicle speed using an Extended Kalman Filter. Prediction of the current gear is based on the ratio of engine and vehicle speeds. The mass of the vehicle can be measured using scales, or alternatively estimated in case significant variations in vehicle mass are expected. Further details on the sensor fusion, gear ratio estimation, and mass estimation are given by Jensen *et al.* (2022a,b). The engine torque $T_e$ during braking is not directly available and needs to be estimated from the available signals.

Regarding the constant model parameters, the wheel mass moment of inertia $I_w$ can for example be approximated based on geometry and material properties (Metz *et al.*, 1990). This leaves the aerodynamic drag $C_a$, rolling resistance $C_r$, and engine mass moment of inertia $I_e$. The aerodynamic drag and rolling resistance can be estimated from coast-down tests of the vehicle with the drivetrain disengaged i.e., transmission in neutral or clutch disengaged. This means the engine torque and mass moment of inertia can be neglected i.e., $T_e = I_e = 0$. Considering this the longitudinal dynamics can be expressed as Eq. (7). The parameters can then be calculated from a linear regression problem $\mathbf{X}^T\phi = \mathbf{y}$.

$$\underbrace{\frac{1}{2}\rho_a \dot{x}^2}_{\mathbf{x}_1}\ \underbrace{C_a}_{\phi_1}\ + \underbrace{mg\cos(\alpha)}_{\mathbf{x}_2}\ \underbrace{C_r}_{\phi_2}\ = \underbrace{-\left(m + I_w\frac{1}{r_w^2}\right)\ddot{x} - mg\sin(\alpha)}_{\mathbf{y}} \tag{7}$$

With the aerodynamic drag and rolling resistance estimated, the terms related to the drivetrain can also be estimated from coast-down tests, but with the drivetrain engaged. Assuming the drivetrain efficiency $\eta_{dt} = 1$ since it will be implicitly included in the engine braking torque model, the braking torque can be expressed as Eq. (8). It is assumed that the torque can be modelled as a linear function of the engine speed $N_e$. In order to also estimate the engine mass moment of inertia, the term related to the inertia can be moved to the right-hand side of the expression resulting in Eq. (9). Again, the coefficients can be fitted using linear regression, where the first two terms on the left-hand side $f(N_e) = c_0 + N_e c_N$ represent the engine braking model.

$$T_{\text{eb}} = \frac{1}{G}\left[\left(m + I_w\frac{1}{r^2} + I_e G^2\right)\ddot{x} + \frac{1}{2}\rho_a C_a \dot{x}^2 + mgC_r\cos(\alpha) + mg\sin(\alpha)\right] = f(N_e) = c_0 + N_e C_N \tag{8}$$

$$\underbrace{c_0}_{\phi_0}\ +\ \underbrace{N_e}_{\mathbf{x}_1}\ \underbrace{c_N}_{\phi_1}\ -\ \underbrace{G\ddot{x}}_{\mathbf{x}_2}\ \underbrace{I_e}_{\phi_2}\ = \underbrace{\frac{1}{G}\left[\left(m + I_w\frac{1}{r^2}\right)\ddot{x} + \frac{1}{2}\rho_a C_a\dot{x}^2 + mg\left(C_r\cos(\alpha) + \sin(\alpha)\right)\right]}_{\mathbf{y}} \tag{9}$$

## Wear model

The wear estimation model is based on the Archard (1953) wear model, shown in Eq. (10).

$$h(t) = kF_n(t)s(t) \tag{10}$$

The equation expresses the wear height $h$ as function of the normal force $F_n$, sliding distance $s$, and wear coefficient $k$. The wear coefficient is assumed constant. Neither of these are however directly available as standard data on a passenger car. Instead, it is proposed to replace the normal force and sliding distance with expressions that can be derived from more readily available data. The sliding distance should be highly correlated with the distance travelled by the vehicle during braking, while the normal force should be related to how hard the vehicle is braking. Based on vehicle longitudinal dynamics, the force from the friction brakes during braking can be estimated, which is then assumed to be correlated with the normal force. The wear equation can then be approximated by Eq. (11), with $F_b^{\text{brk}}$ being the longitudinal force from the friction brakes and $d^{\text{brk}}$ being the vehicle distance travelled during braking. Finally, the wear coefficient $k$ will need to be fitted to wear measurement data.

$$h(t) = kF_n(t)s(t) \approx kF_b^{\text{brk}}(t)d^{\text{brk}}(t) \tag{11}$$

By rearranging the longitudinal dynamics model in Eq. (1), the force from the friction brakes can then be estimated as Eq. (12), assuming that it is known when the friction brakes are being applied.

$$F_b^{\text{brk}} = \eta_{dt}T_e G - \left(m + I_w\frac{1}{r^2} + I_e G^2\right)\ddot{x} - \frac{1}{2}\rho_a C_a\dot{x}^2 - mg\left[C_r\cos(\alpha) + \sin(\alpha)\right] \tag{12}$$

Inserting the above expression into the wear expression of Eq. (11), along with the expression for the engine braking torque, the resulting wear expression can then be written as

$$h(t) \approx k\left[\left(c_0 + N_e C_N\right)G(t) - \left(m + I_w\frac{1}{r^2} + I_e G(t)^2\right)\ddot{x}(t) - \frac{1}{2}\rho_a C_a\dot{x}(t)^2 - mg\left[C_r\cos(\alpha(t)) + \sin(\alpha(t))\right]\right]d^{\text{brk}}(t) \tag{13}$$

# EXPERIMENTAL RESULTS

## Data acquisition

Usage data was sampled using a sensor unit mounted in the trunk of a typical modern passenger car. The car has a 4-cylinder turbocharged petrol engine and 7-speed dual clutch automatic transmission. The vehicle was weighed on scales at 1,580 kg with a full tank of petrol and including the driver. The tire radius was calculated to be $r = 0.32$ m based on specifications. Wheel mass moment of inertia of $I_w = 4.0$ kgm$^2$ was used, along with air density $\rho_a = 1.2$ kg/m$^3$ and gravitational acceleration $g = 9.81$ m/s$^2$. Gearing ratios are listed in Tab. 1.

**Table 1 – Vehicle differential and transmission gearing ratios.**

| Differential | Gear 1 | Gear 2 | Gear 3 | Gear 4 | Gear 5 | Gear 6 | Gear 7 |
|---|---|---|---|---|---|---|---|
| 4.234 | 3.188 | 2.190 | 1.517 | 1.057 | 0.738 | 0.557 | 0.433 |

The sensor unit consists of a 6-axis IMU providing accelerations and angular velocities, a GNSS module providing vehicle positions, and OBD-II connectivity. IMU data was sampled at 200 Hz, OBD-II at 4 Hz, and GNSS at 1 Hz. The three data sources were fused to provide more accurate vehicle state estimations, including vehicle attitude angles. Sensor fusion output was then low-pass filtered and down-sampled from 200 Hz to 4 Hz, to match the OBD-II data. From OBD-II only the engine speed, vehicle speed, and engine load parameters were used. Engine and vehicle speeds were used for the gear predictions. Engine speed was also used for the engine braking torque model of Eq. (8), while vehicle speed was also used in the aerodynamic drag term of the longitudinal dynamics model. The engine load parameter was used to determine when the throttle was not being used, to indicate when the braking state estimations of Eq. (4) should be carried out.

## Vehicle coast-down tests

A test drive was carried out for estimation of vehicle drag parameters and engine braking. A series of measurements were performed where the vehicle was allowed to slow down without the use of the friction brakes. Tests were first carried out with the drivetrain disengaged, allowing for estimation of aerodynamic drag and rolling resistance using Eq. (7). This was then followed by coast-downs with the drivetrain engaged and in different gears, to allow for estimation of engine braking using Eq. (9). The tests were performed on public roads, following local traffic laws. The resulting estimated model parameters are listed in Tab. 2. The values of both the aerodynamic drag and rolling resistance coefficients agree well with values estimated on the same vehicle using a different approach by Jensen *et al.* (2022b). The aerodynamic drag is slightly higher than values of around $C_dA_0 = 0.6$ m$^2$ of online sources (Automobile Catalog, 2022). The rolling resistance coefficient is around the expected value for a passenger car (Gillespie, 1992, ch. 4).

**Table 2 – Estimated model parameters from coast-down tests.**

| Parameter | $C_dA_0$ [m$^2$] | $C_r$ | $I_e$ [kgm$^2$] | $c_N$ [Nm/RPM] | $c_0$ [Nm] |
|---|---|---|---|---|---|
| Estimate | 0.73 | 0.012 | 0.48 | -0.00677 | -18.70 |

Based on these parameter estimates, Fig. 1 shows a comparison of measured and estimated longitudinal vehicle accelerations against vehicle speeds, without application of friction brakes and both with and without drivetrain engaged. Fig. 2 shows a similar comparison, but against time. The effect of the drivetrain on the deceleration can clearly be observed, with significantly greater deceleration across all gears. It can also be seen that the estimated acceleration appears to fit the measurements very well with the drivetrain disengaged, across the full range of vehicle speeds from around 9-33 m/s. With the drivetrain engaged the estimates also match the measurements very well in gears 1 through 5. However, discrepancies are present in gears 6 and 7. It can be seen that the measured acceleration in gears 5, 6, and 7 are very similar, which is unexpected based on the effect of the gear ratios. It is thought that this could be caused by the engine control strategy, in order to achieve a certain minimum deceleration independent on the current gear. It was decided not the investigate this discrepancy further, as model discrepancies are to be considered when tuning the braking state predictor sensitivity parameter $\beta$.

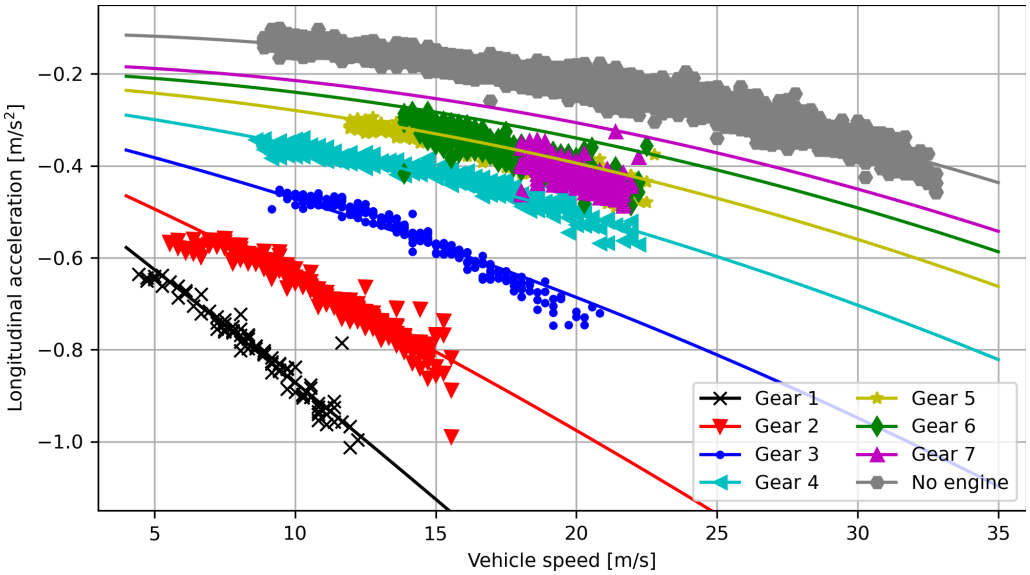


**Figure 1 – Comparison of measured and estimated coasting acceleration i.e., no friction brakes and closed throttle against vehicle speed. Both with and without drivetrain engaged and using estimated parameters from Tab. 2.**

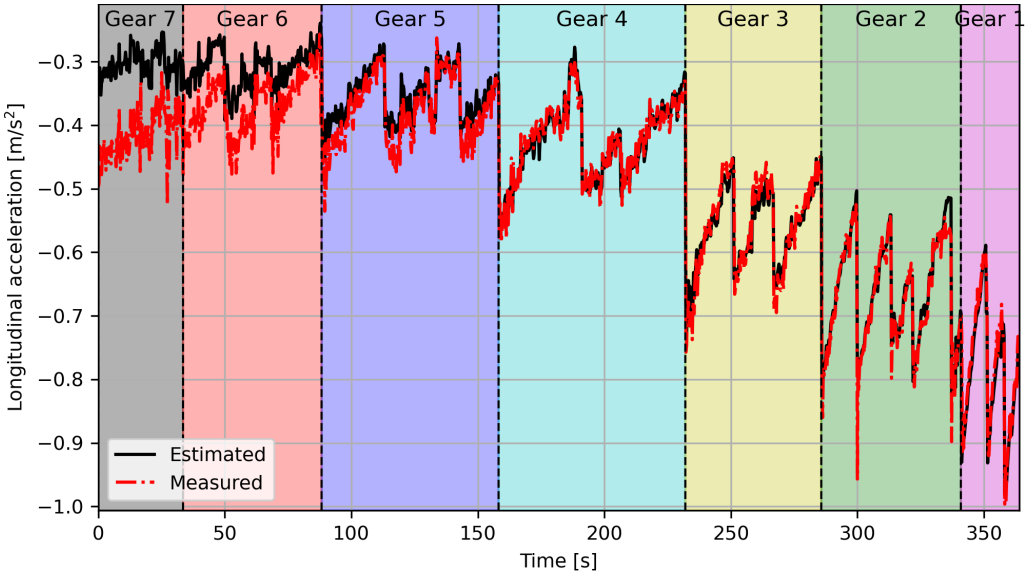


**Figure 2 – Comparison of measured and estimated coasting acceleration i.e., no friction brakes and closed throttle against time. Both with and without drivetrain engaged and using estimated parameters from Tab. 2. Note that the shown samples were extracted to only show samples during braking, with the resulting jumps in time being excluded.**

## Vehicle braking state prediction

Having obtained the model for the vehicle coasting acceleration, the vehicle braking state model of Eq. (4) is to be fitted and validated. For this two additional test drives were carried out: (I) and (II). The first (I) was used for fitting of the sensitivity $\beta$ and the other (II) for validation. In order to obtain labels of when the vehicle brakes were being engaged, a camera was used to record the brake pedal of the car during the drives. Using object tracking to track the movement of the brake pedal, it was assumed that the brakes were being engaged when the brake pedal had moved a certain distance.

A threshold of $\beta = 0.409$ was obtained by training on the first dataset (I), while a value of $\beta = 0.338$ was obtained by training on the other dataset (II). A confusion matrix has been constructed and is shown in Fig. 3, for the case with training on (I) and validating on (II) i.e., using $\beta = 0.409$. A confusion matrix compares predicted and true classifications for each sample. It can be seen that the predictor generally performs well, with very few false positives, but slightly more false

negatives. The false negatives are believed to be caused mainly by the large number of non-braking samples compared to the number of braking samples. The sensitivity was trained to maximize accuracy i.e., number of correct predictions. Due to the large unbalance of braking states, the predictor is trained to have a lower sensitivity in order to correctly classify the large number of non-braking samples. However, this is not believed to be a significant problem, as the misclassifications mainly appear during low vehicle deceleration, where brake pad wear is also low.

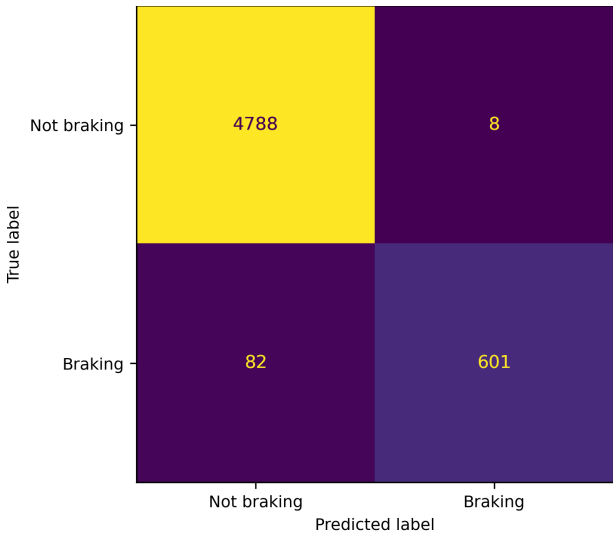


**Figure 3 – Confusion matrices for dataset (II) using sensitivity value from training on dataset (I).**

## Brake pad wear estimation

Wear data was obtained through measurements of the outer brake pad at the front left of the vehicle. A micrometer screw was used to measure the thickness at three locations: leading edge, center, and trailing edge. For consistency all measurements were taken approximately in the center of the pad along the radial direction. A total of 16 measurements were carried out over approximately 5,000 km and considering different driving conditions. Approximately 0.75 mm of brake pad thickness was worn during the tests. The thickness is lowest at the trailing edge, followed by the center, and then the leading edge.

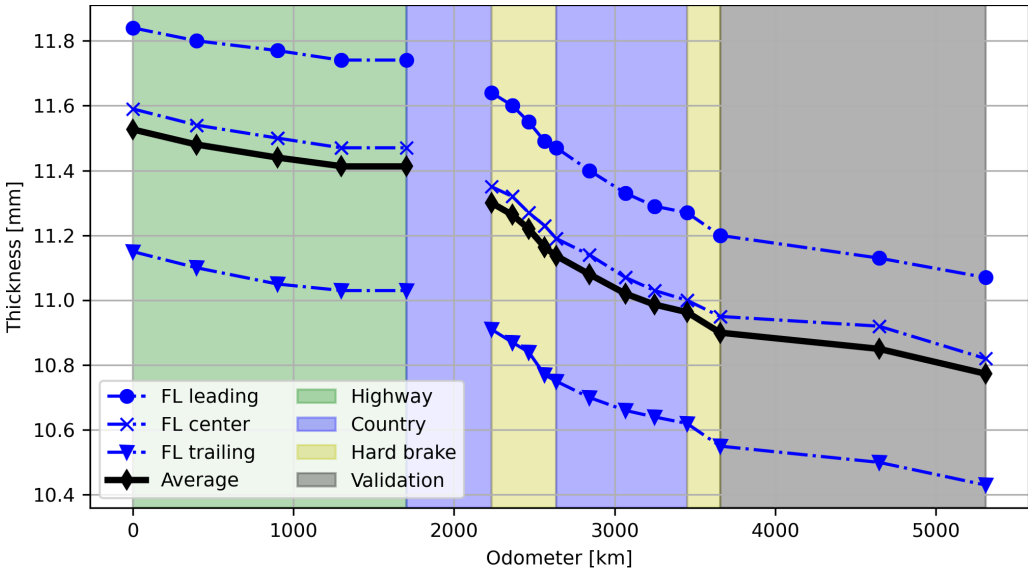


**Figure 4 – Measured wear at leading edge, center, and trailing edge of outer pad at front left wheel against distance travelled. Background colored according to primary driving type.**

The wear is modelled using Eq. (13) with distance travelled $d$ from the sensor fusion state estimation and braking

force $F_b$ from Eq. (12), while the braking state is predicted using Eq. (4). Using the average across the three measurement locations of the brake pad as targets, the wear coefficient $k$ is estimated with the resulting fit shown in Fig. 5. It can be seen that the model fits the measurements very well with $R^2 = 0.97$, but with the final two measurements deviating slightly. For further validation of the proposed method, data over longer periods and with higher wear is required. Additionally, wear from other pads, both on the same and other vehicles, also needs to be considered. The method could then be used for prediction of remaining useful life of the brake pads based on usage, allowing for predictive maintenance.

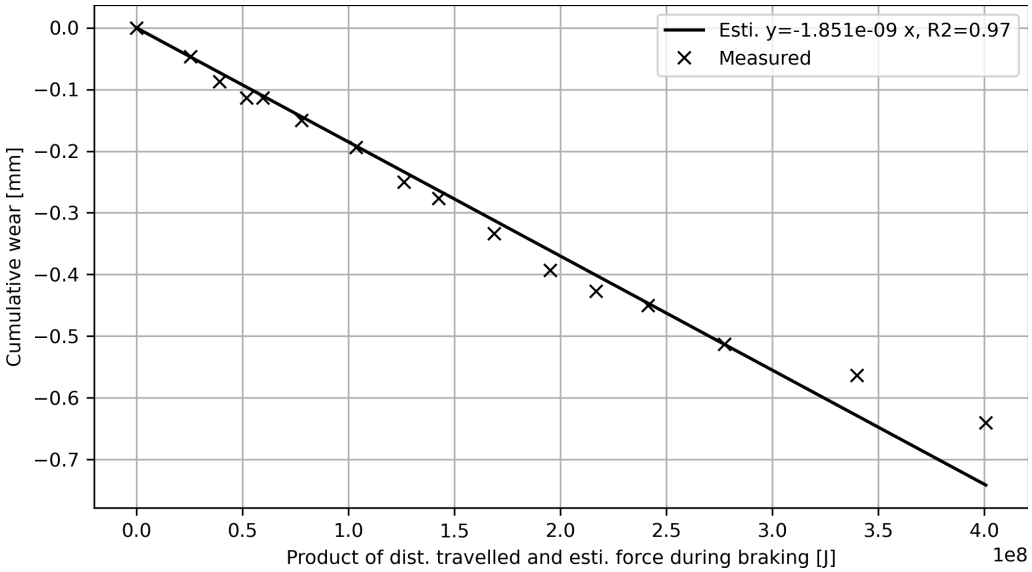


**Figure 5 – Estimated wear from linear regression and measured wear averaged across the three measurement locations of outer front left brake pad.**

## CONCLUSION

The problem of estimating brake pad wear of passenger cars has been considered. The proposed method is based on vehicle longitudinal dynamics, using IMU, GNSS, and standard vehicle OBD data. This ensures the method can be easily applied to a wide range of vehicles, as it does not rely on manufacturer specific data from the CAN-bus. The paper covers four parts: (I) estimation of vehicle drag, (II) estimation of engine braking, (III) prediction of vehicle braking state, and (IV) estimation of brake pad wear. Comparison of estimated and measured accelerations show good agreements for (I) and (II). Using braking state labels obtained from a camera recording the brake pedal to train and validate the braking state predictor, also results in good agreements with high prediction accuracy. The predictor however gives a number of false negatives, attributed to the large unbalance in the data labels used for training. For the final part (IV), brake pad measurement data has been used to train a linear model, depending only on the product between distance travelled and longitudinal braking force during braking. The model fits the data very well with $R^2$ of 0.97, but with some slight deviations appearing for the final measurements. More data is needed for further validation, in order to see how well the model performs over a greater range of wear, to allow for accurate wear predictions to be made in the future.

## REFERENCES

Archard, J.F., 1953. "Contact and rubbing of flat surfaces". *Journal of Applied Physics*, Vol. 24, pp. 981–988.

Automobile Catalog, 2022. "2018 audi a4 2.0 tfsi ultra s-tronic specifications". `https://www.automobile-catalog.com/car/2018/2222855/audi_a4_2_0_tfsi_ultra_190_s-tronic.html`. Accessed October 31 2022.

Cliff, W.E. and Bowler, J.J., 1998. "The measured rolling resistance of vehicles for accident reconstruction". *SAE Technical Paper 980368*.

Gailis, M. and Berjoza, D., 2012. "On prediction of motor vehicle brake pad wearout". In *Proceedings of 11th International Scientific Conference on Engineering for Rural Development*. Jelgava, Latvia, pp. 349–354.

Gillespie, T., 1992. *Fundamentals of Vehicle Dynamics*. SAE International.

Hendricks, E. and Sorenson, S., 1990. "Mean value modelling of spark ignition engines".

Jensen, K.M., Santos, I.F., Clemmensen, L.H.K., Theodorsen, S. and Corstens, H.J.P., 2022a. "Mass estimation of ground vehicles based on longitudinal dynamics using imu and can-bus data". *Mechanical Systems and Signal Processing*, Vol. 162.

Jensen, K.M., Santos, I.F., Clemmensen, L.H.K., Theodorsen, S. and Corstens, H.J.P., 2022b. "Mass estimation of ground vehicles based on longitudinal dynamics using loosely coupled integrated navigation system and can-bus data with model parameter estimation". *Mechanical Systems and Signal Processing*, Vol. 171.

Kijanski, J., Otto, J., Stebner, F., Weber, J., Franke, R. and Ostermeyer, J.P., 2020. "Investigation of influence on brake pad wear". *SAE Technical Paper 2020-01-1614*.

Limpert, R., 2011. *Brake Design and Safety, 3rd Ed.* SAE International.

Liu, T. and Rhee, S.K., 1978. "High temperature wear of semimetallic disc brake pads". *Wear*, Vol. 46, No. 1, pp. 213–218.

Metz, L.D., Akouris, C.K., Ayrey, C.S., Clark, M.C. and Agney, C.S., 1990. "Moments of inertia of mounted and unmounted passenger car and motorcycle tires". *SAE Transactions*, Vol. 99, pp. 1079–1085.

Rajesh, P.K., Manikandan, N., Ramshankar, C.S., Vishwanathan, T. and Sathishkumar, C., 2019. "Digital twin of an automotive brake pad for predictive maintenance". *Procedia Computer Science*, Vol. 165, pp. 18–24.

Tiedemann, M., Kijanski, J., Otto, J. and Ostermeyer, G.P., 2020. "Prediction of brake pad wear in battery-electric vehicles". *ATZ Worldwide*, Vol. 122, No. 6, pp. 26–31.

White, K., Merala, R., Desautels, D. and Ellis-Caleo, T., 2012. "Rollout deceleration of modern passenger vehicles". *SAE Technical Paper 2012-01-0616*.

White, R. and Korst, H., 1972. "The determination of vehicle drag contributions from coast-down tests". *SAE Transactions*, Vol. 81, pp. 354–359.

Zhang, S., Hao, Q., Liu, Y., Jin, L., Ma, F., Sha, Z. and Yang, D., 2019. "Simulation study on friction and wear law of brake pad in high-power disc brake". *Mathematical Problems in Engineering*, Vol. 2019, No. 2, pp. 1–15.

## RESPONSIBILITY NOTICE

The author(s) is (are) the only responsible for the printed material included in this paper.